Nonlinear Robust Control Design for a Planar Robot Arm

Zeki Okan Ilhan[1]

[1]McCoy School of Engineering, Midwestern State University, 3410 Taft Blvd, Wichita Falls, TX, 76308, USA, {zeki.ilhan@msutexas.edu}

ABSTRACT

1 Introduction

This work aims to conduct a comprehensive analysis of the kinematics, dynamics, motion planning, and nonlinear control design for a basic two-link planar robot arm (Fig. 1). As interest in robotics continues to grow, the two-link arm remains fundamental for the development and control of more advanced serial robotic manipulators [1] and humanoid robots [2]. In this study, the system dynamic model is first developed using Lagrange's equations [3] in a non-conservative format. Additionally, an inverse kinematic analysis is conducted to determine the target joint variables for executing circular motion in the task plane. The dynamic model is then integrated with a feedback controller based on the nonlinear, Sliding Mode Control (SMC) strategy [4]. The tracking performance of the proposed controller is tested in closed-loop numerical simulations, in which the target trajectories are set to the joint variables obtained from the inverse kinematic study. Furthermore, the dynamic model is slightly altered in the simulation by adding 5% extra weights to the links in order to assess the controller's robustness against external disturbances.

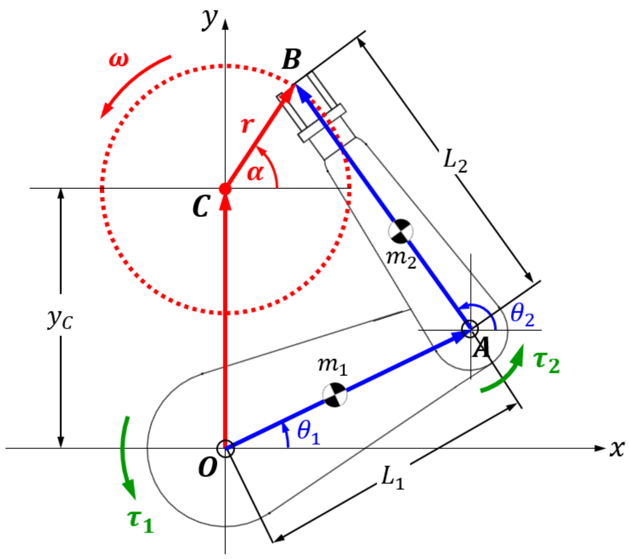

Figure 1: A sketch of the 2-link (RR) planar robot

Table 1: A list of the model parameters

Parameter	Value	Description
L_1, L_2	0.50 m	Lengths of the links
L_{m_1}, L_{m_2}	0.25 m	CoM lengths of the links
m_1, m_2	3.00 kg	Masses of the links
I_1, I_2	0.25 kg·m²	Moments of inertias of the links
r	0.25 m	Radius of the circular path
ω	100 °/s	End-effector rotational speed
x_C	0.00 m	Abscissa of the center point, C.
y_C	0.50 m	Ordinate of the center point, C.
$\theta_1(t), \theta_2(t)$	–	Angular positions of the links
$\tau_1(t), \tau_2(t)$	–	Torque inputs on the joints

2 Dynamic Model

Lagrange's equations are applied in a non-conservative format to develop the dynamic model for a torque input scenario. As Lagrange modeling relies on energy principles, it was essential to derive the expressions for the total kinetic and potential energy of the robot, along with the total work done by the non-conservative factors such as the torque inputs. By selecting angles θ_1 and θ_2 (Fig. 1) as the independent generalized coordinates, the dynamic model can be written compactly in the following matrix form [3]:

$$\begin{bmatrix} A_{11} & A_{12} \\ A_{21} & A_{22} \end{bmatrix} \begin{bmatrix} \ddot{\theta}_1(t) \\ \ddot{\theta}_2(t) \end{bmatrix} + \begin{bmatrix} 0 & B_{12} \\ B_{21} & 0 \end{bmatrix} \begin{bmatrix} \dot{\theta}_1^2(t) \\ \dot{\theta}_2^2(t) \end{bmatrix} + \begin{bmatrix} c_1 \\ c_2 \end{bmatrix} = \begin{bmatrix} \tau_1(t) \\ \tau_2(t) \end{bmatrix} \tag{1}$$

where, the elements of the matrices A, B, c in (1) are related to the link inertia, geometry and joint variables (Table 1) as follows:

$$A_{11} = I_1 + m_2 L_1^2 \tag{2}$$

$$A_{12} = A_{21} = m_2 L_1 L_{m_2} \cos(\theta_1 - \theta_2) \tag{3}$$

$$A_{22} = m_2 L_{m_2}^2 + I_2 \tag{4}$$

$$B_{12} = -B_{21} = m_2 L_1 L_{m_2} \sin(\theta_1 - \theta_2) \tag{5}$$

$$c_1 = \left(m_1 g L_{m_1} + m_2 g L_1\right) \cos\theta_1 \tag{6}$$

$$c_2 = m_2 g L_{m_2} \cos\theta_2 \tag{7}$$

DOI: 10.17185/duepublico/82637

3 Inverse Kinematic Analysis

One possible configuration of the robot for this motion plan is sketched in Fig. 1. Forming a vector chain along the links ($\overrightarrow{OA} + \overrightarrow{AB}$), and a separate vector chain avoiding the links ($\overrightarrow{OC} + \overrightarrow{CB}$), a Loop Closure Equation (LCE) could be obtained. Separation of the horizontal and vertical components of the LCE leads to the following two nonlinear equations for the joint variables (θ_1, θ_2):

$$L_1 \cos\theta_1 + L_2 \cos\theta_2 = r\cos\alpha(t) \tag{8}$$

$$L_1 \sin\theta_1 + L_2 \sin\theta_2 = y_C + r\sin\alpha(t) \tag{9}$$

where, $\alpha(t) = \omega t$ assuming a constant rotational speed, ω while tracing the circle. The time evolution of the angular positions (θ_1, θ_2) of the links are obtained and plotted in Fig. 2 as the "target" trajectories to achieve in the closed-loop control simulations.

4 Sliding-Mode Control Design and Simulation Results

To initiate control design, the Lagrange model (1) is first re-organized in the following explicit form:

$$\ddot{\Theta}(t) = f(\Theta, \dot{\Theta}, t) + u(t) \tag{10}$$

where, $\Theta = [\theta_1 \quad \theta_2]^T$ is the state vector, $f(\Theta, \dot{\Theta}, t) = -A^{-1}B\dot{\Theta}^2 - A^{-1}c$, and $u(t) = A^{-1}\tau(t)$ is the control input. To quantify the tracking performance, a cost function is also defined by combining position tracking error and velocity tracking error as follows:

$$e(t) = \left(\dot{\Theta} - \dot{\Theta}_d\right) + \lambda(\Theta - \Theta_d) \ , \ \ (\lambda > 0) \tag{11}$$

where, Θ_d refers to the desired (target) trajectories. Note that error-free tracking implies: $e = 0$ (or, $\dot{e} = 0$). Hence, after taking the first derivative of (11), and then substituting the dynamic model (10), the control input $u(t)$ is obtained as follows:

$$u(t) = \ddot{\Theta}_d - f\left(\Theta, \dot{\Theta}, t\right) - \lambda\left(\dot{\Theta} - \dot{\Theta}_d\right) - K\mathrm{sat}[e(t)/\phi] \tag{12}$$

The last term on the right side of (12) is added to provide state feedback action to enable control switching for robustness. The saturation function eliminates input chattering due to repetitive switching action especially when the states are very close to their respective targets [4]. The results of the closed-loop control simulation are provided in Figs. 2-3. Perfect tracking is achieved despite the 5% increase on the link masses, which validates the robustness of the proposed control law against external disturbances.

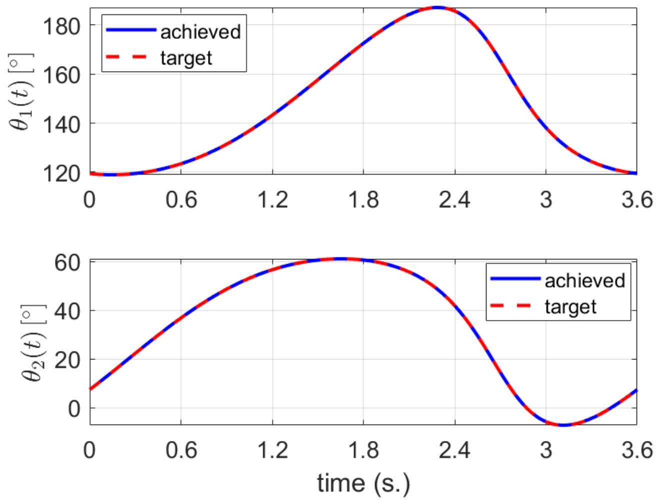

Figure 2: Time evolution of the joint variables

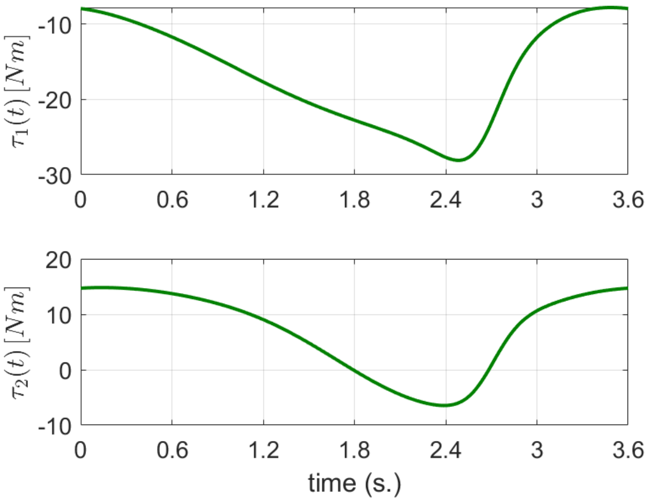

Figure 3: Time evolution of the torque inputs

References

[1] M. K. Ozgoren, *Kinematics of General Mechanical Systems.* Wiley, 2020.

[2] V. De-León-Gómez et al. "A procedure to find equivalences among dynamic models of planar biped robots", *Simulation Modelling Practice and Theory,* vol. 75, pp. 48-66, 2017.

[3] Z. Ilhan, "Benchmarking various nonlinear control design techniques for a two-link planar robot arm", in *Proceedings of the ASME 2022 International Mechanical Engineering Congress and Exposition*. Columbus, OH, USA. 2022.

[4] J-J. E. Slotine and W. Li, *Applied Nonlinear Control*. Prentice Hall, 1991.

DOI: 10.17185/duepublico/82637
URN: urn:nbn:de:hbz:465-20241118-135204-1

1st IFToMM Young Faculty Group Symposium on Emerging Fields in Mechanism and Machine Science 2024: 19.11. - 21.11.2024, Online Symposium